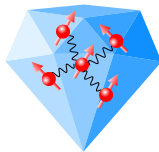


Cross-relaxation in dense ensembles of NV centers and application to magnetometry

Clément Pellet-Mary PhD Defense



LPENS
LABORATOIRE DE PHYSIQUE
DE L'ÉCOLE NORMALE SUPÉRIEURE



SORBONNE
UNIVERSITÉ



Université
de Paris

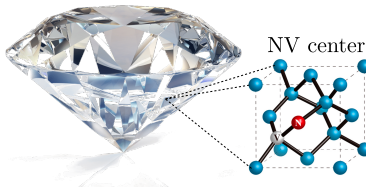


QUANTERA



institut
universitaire
de France

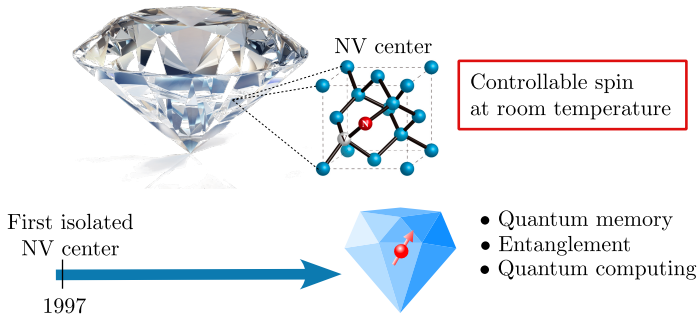
Context of my PhD



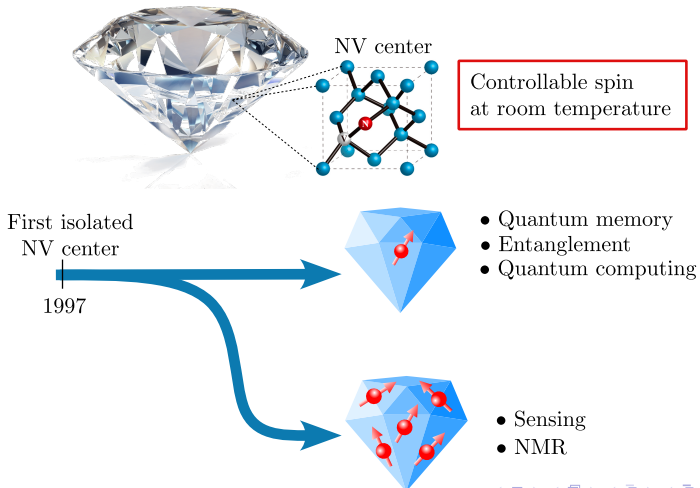
NV center

Controllable spin
at room temperature

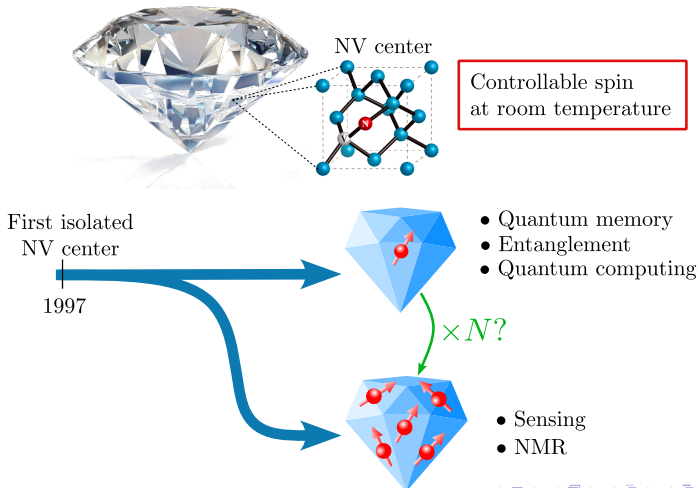
Context of my PhD



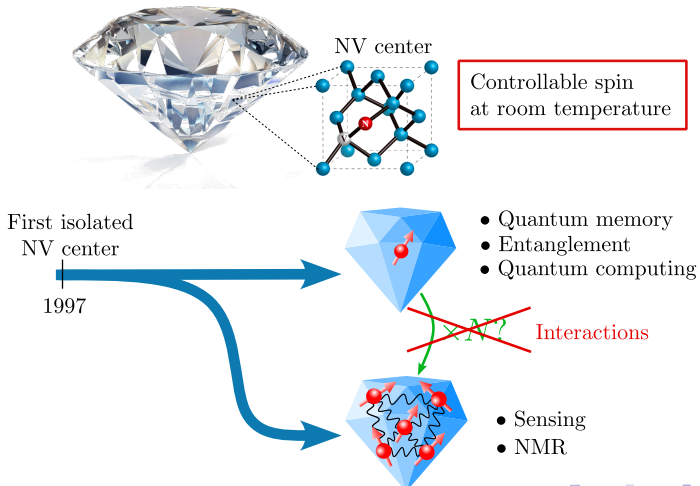
Context of my PhD



Context of my PhD



Context of my PhD



Outline

Sensing with quantum mechanics

NV center spin properties

Low field depolarization magnetometry (LFDM)

Depolarization mechanisms in dense NV ensemble

Outline

Sensing with quantum mechanics

NV center spin properties

Low field depolarization magnetometry (LFDM)

Depolarization mechanisms in dense NV ensemble

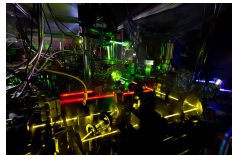
Quantum sensing and metrology

Quantum metrology:

Using quantum* properties to create
more sensitive measurement protocols.

* quantum \equiv discrete energy levels

Time measurement



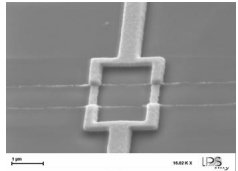
Atomic clock

Medical imaging



MRI

Magnetometry

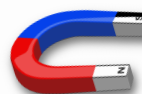
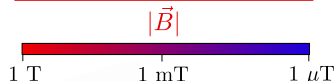


SQUIDs

Key properties of magnetometers

Sensitivity [T/ $\sqrt{\text{Hz}}$]:

Minimum magnetic field value detectable with a signal-to-noise ratio of 1 within 1 second.



Magnetic source

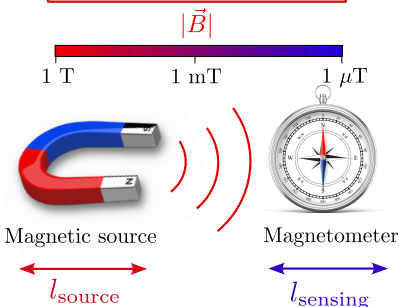


Magnetometer

Key properties of magnetometers

Sensitivity [T/ $\sqrt{\text{Hz}}$]:

Minimum magnetic field value detectable with a signal-to-noise ratio of 1 within 1 second.



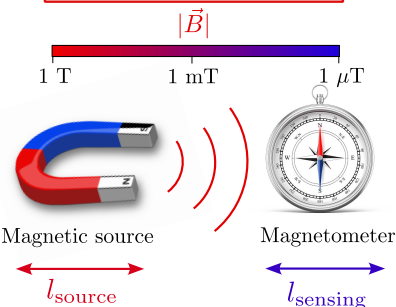
Optimum spatial resolution (imaging):

$$l_{\text{sensing}} \leq l_{\text{source}}$$

Key properties of magnetometers

Sensitivity [T/ $\sqrt{\text{Hz}}$]:

Minimum magnetic field value detectable with a signal-to-noise ratio of 1 within 1 second.



Optimum spatial resolution (imaging):

$$l_{\text{sensing}} \leq l_{\text{source}}$$

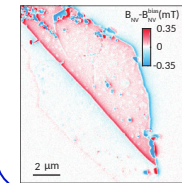
Magnetoencephalography



$$|\vec{B}| \sim 10 \text{ fT}$$

$$l \sim 1 \text{ cm}$$

2D materials magnetism

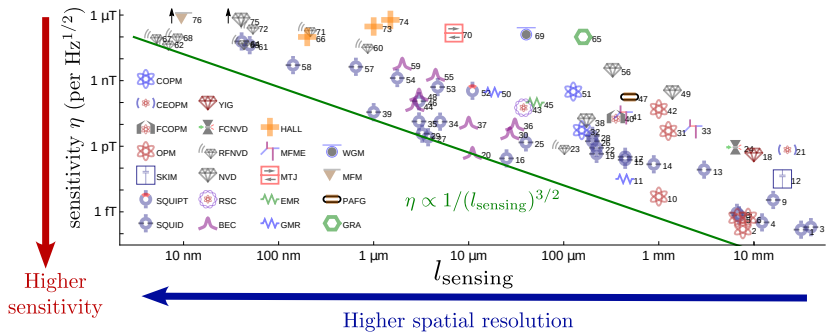


$$|\vec{B}| \sim 100 \mu\text{T}$$

$$l \sim 50 \text{ nm}$$

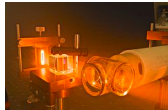
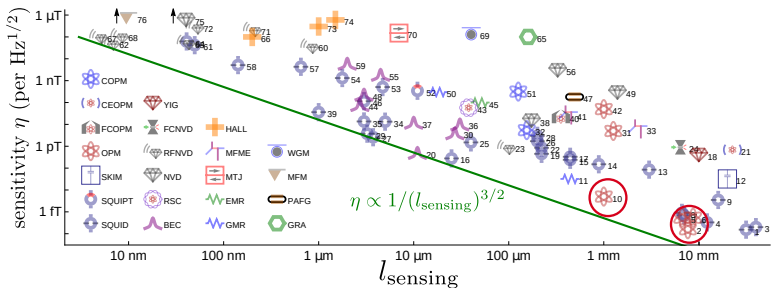
Thiel, L. et al (2019). Science, 364(6444), 973-976.

Sate of the art magnetometers



Mitchell, M. W., & Alvarez, S. P. (2020). Reviews of Modern Physics, 92(2), 021001

Sate of the art magnetometers



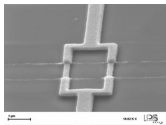
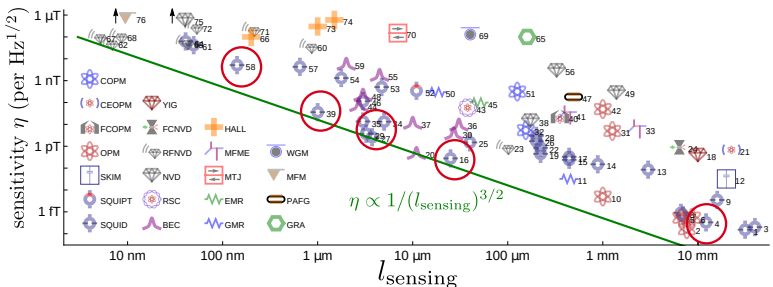
Optically pumped magnetometers (OPM)

✓ Very high sensitivity

✗ Limited in size

Mitchell, M. W., & Alvarez, S. P. (2020). Reviews of Modern Physics, 92(2), 021001

State of the art magnetometers



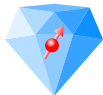
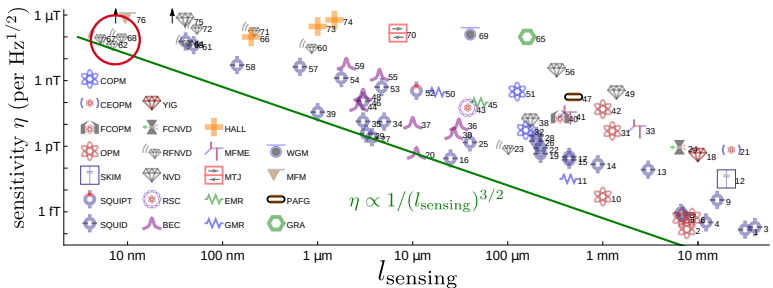
Superconducting quantum interference device (SQUID)

✓ High versatility, mature technology

✗ Requires cryogenic temperatures

Mitchell, M. W., & Alvarez, S. P. (2020). *Reviews of Modern Physics*, 92(2), 021001

State of the art magnetometers

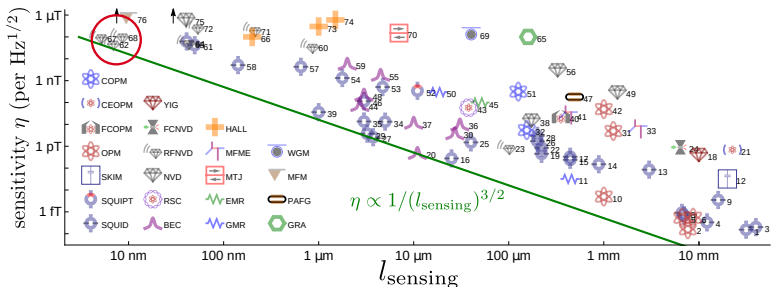


(Single) NV center

- nm resolution
 - Room temperature

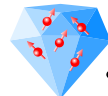
Mitchell, M. W., & Alvarez, S. P. (2020). *Reviews of Modern Physics*, 92(2), 021001.

State of the art magnetometers



(Single) NV center

- nm resolution
- Room temperature

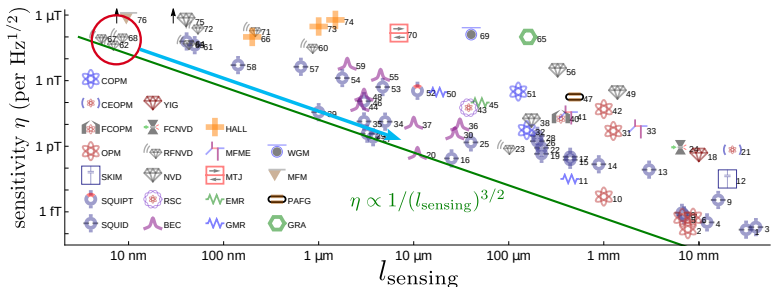


NV ensemble

- μm resolution
- Room temperature
- Higher sensitivity

Mitchell, M. W., & Alvarez, S. P. (2020). *Reviews of Modern Physics*, 92(2), 021001

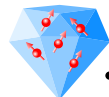
State of the art magnetometers



(Single) NV center

- nm resolution
- Room temperature

$$\eta \propto 1/\sqrt{N} \propto 1/\sqrt{V}$$

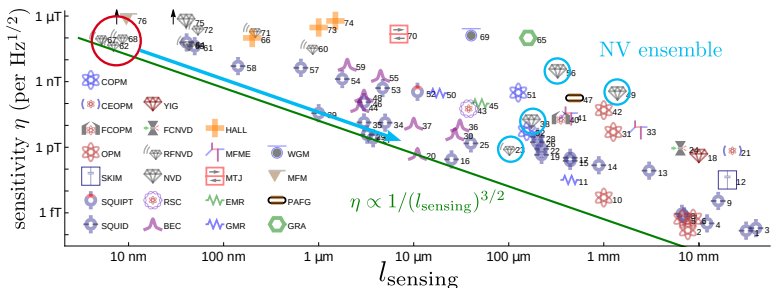


NV ensemble

- μm resolution
- Room temperature
- Higher sensitivity

Mitchell, M. W., & Alvarez, S. P. (2020). *Reviews of Modern Physics*, 92(2), 021001

State of the art magnetometers



(Single) NV center

- nm resolution
 - Room temperature

~~$\eta \propto 1/\sqrt{N} \propto 1/\sqrt{V}$~~

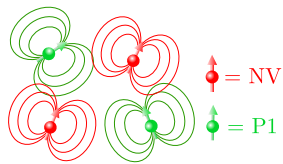
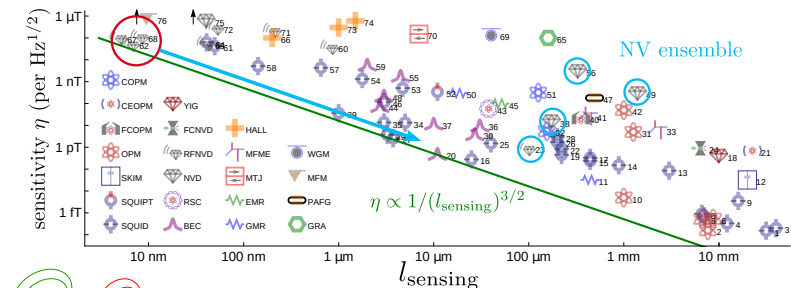
Interactions

NV ensemble

- μm resolution
 - Room temperature
 - Higher sensitivity

Mitchell, M. W., & Alvarez, S. P. (2020). *Reviews of Modern Physics*, 92(2), 021001.

State of the art magnetometers

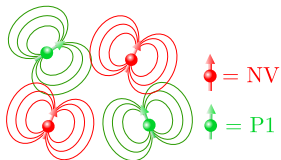
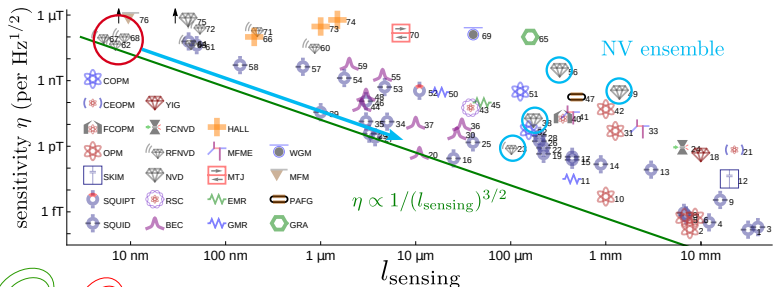


Interactions:

- Spectral broadening
- Modified spin dynamics

Mitchell, M. W., & Alvarez, S. P. (2020). *Reviews of Modern Physics*, 92(2), 021001

State of the art magnetometers



Interactions:

- Spectral broadening
- Modified spin dynamics

Solutions:

- Decoupling interactions (Hamiltonian engineering)
- Exploiting interactions

Mitchell, M. W., & Alvarez, S. P. (2020). *Reviews of Modern Physics*, 92(2), 021001

Outline

Sensing with quantum mechanics

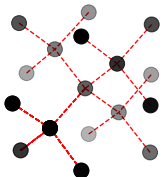
NV center spin properties

Low field depolarization magnetometry (LFDM)

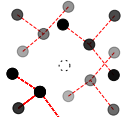
Depolarization mechanisms in dense NV ensemble

Colored centers in diamond

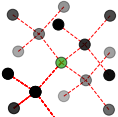
Diamond crystal lattice



Point-like defects



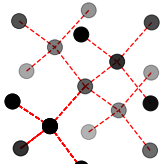
Vacancy



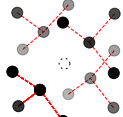
Substitution

Colored centers in diamond

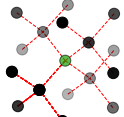
Diamond crystal lattice



Point-like defects

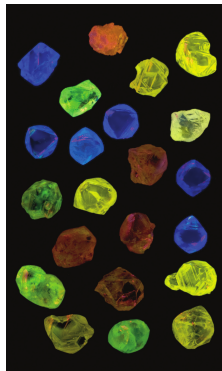
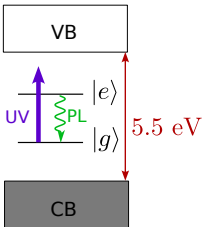


Vacancy



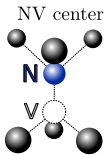
Substitution

Colored center fluorescence

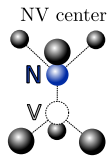


Natural diamonds fluorescence under UV light

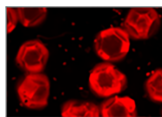
Synthetic diamond and NV centers



Synthetic diamond and NV centers



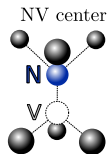
High Pressure High Temperature
(HPHT)



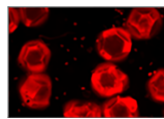
Adamas 15/150 μm

$[\text{NV}] \approx 3 \text{ ppm}$

Synthetic diamond and NV centers



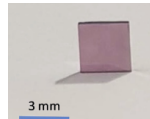
High Pressure High Temperature
(HPHT)



Adamas 15/150 μm

$[\text{NV}] \approx 3 \text{ ppm}$

Chemical Vapour Deposition
(CVD)

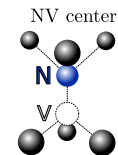


IRCP-LSPM

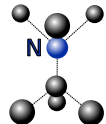
$[\text{NV}] \approx 4.5 \text{ ppm}$

Tallaire, A., et al (2020). Carbon, 170, 421-429.

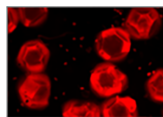
Synthetic diamond and NV centers



N_s (P1 center)



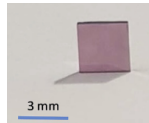
High Pressure High Temperature
(HPHT)



Adamas 15/150 μm

$[\text{NV}] \approx 3 \text{ ppm}$
 $[\text{P1}] \approx 100 \text{ ppm}$

Chemical Vapour Deposition
(CVD)

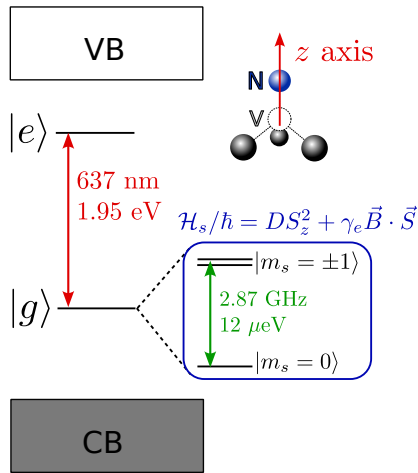


IRCP-LSPM

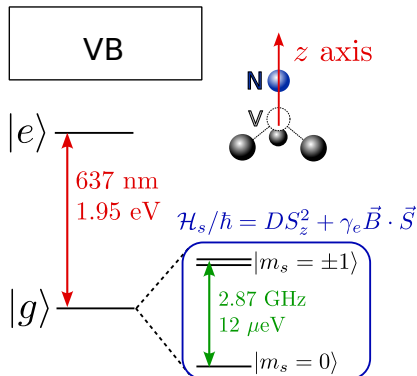
$[\text{NV}] \approx 4.5 \text{ ppm}$
 $[\text{P1}] \approx 25 \text{ ppm}$

Tallaire, A., et al (2020). Carbon, 170, 421-429.

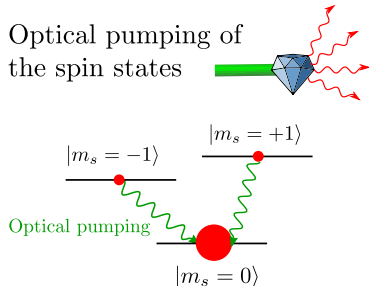
The NV center energy levels



The NV center energy levels

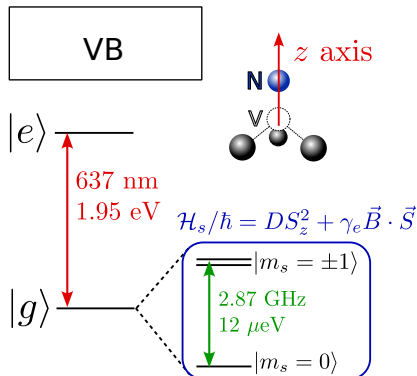


Optical pumping of the spin states

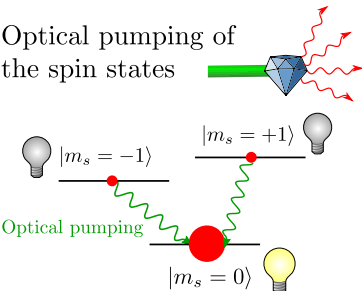


- Population accumulation in the $|0\rangle$ state
 - ↳ Initialization of the spin state

The NV center energy levels

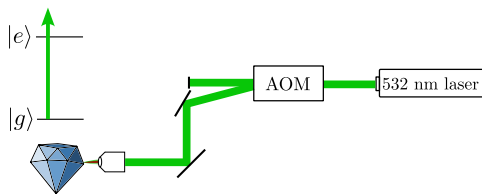


Optical pumping of the spin states

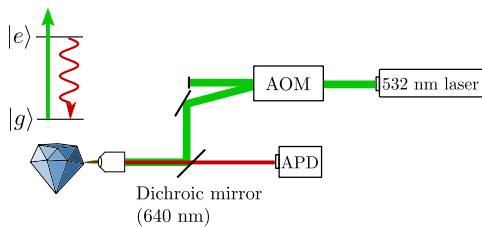


- Population accumulation in the $|0\rangle$ state
 - ↳ Initialization of the spin state
- $|0\rangle$ state brighter than $|\pm 1\rangle$ states
 - ↳ Optical readout of the spin state

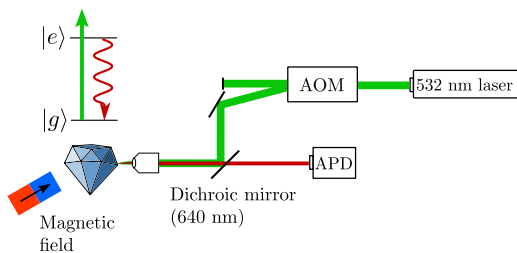
Experimental setup



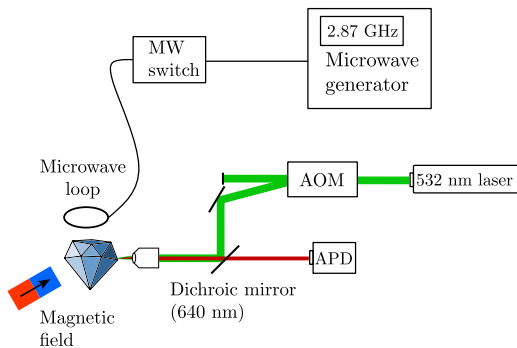
Experimental setup



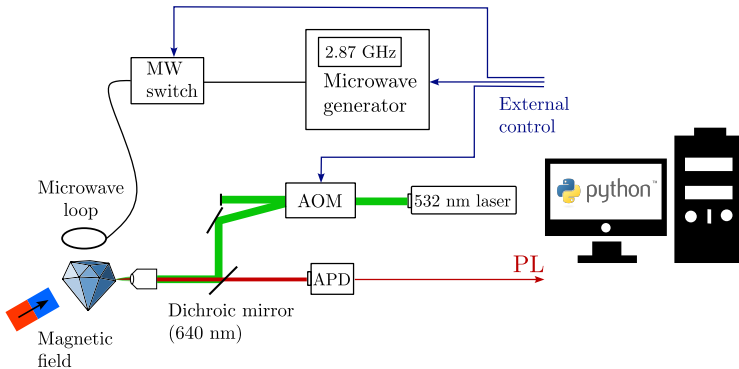
Experimental setup



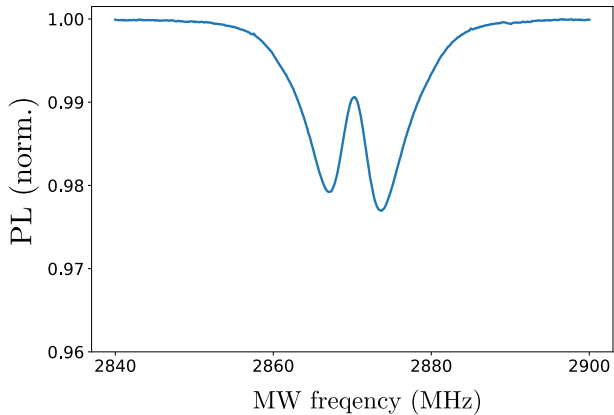
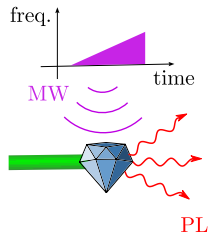
Experimental setup



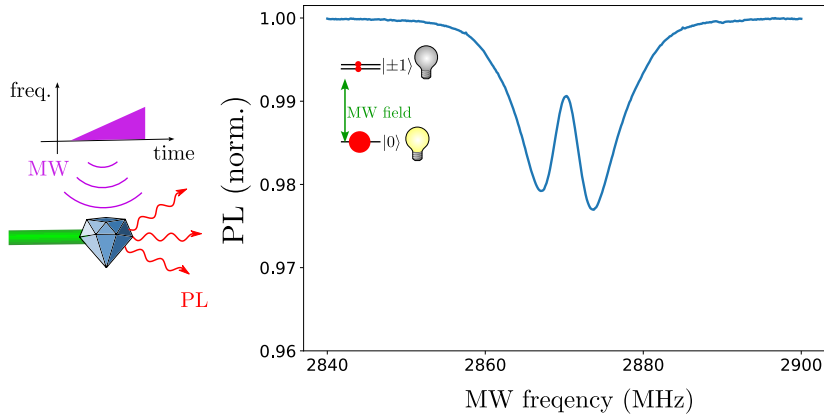
Experimental setup



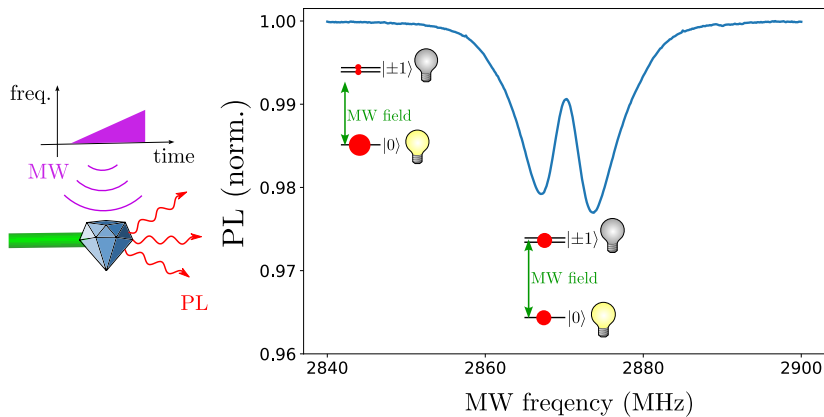
Optically detected magnetic resonance (ODMR)



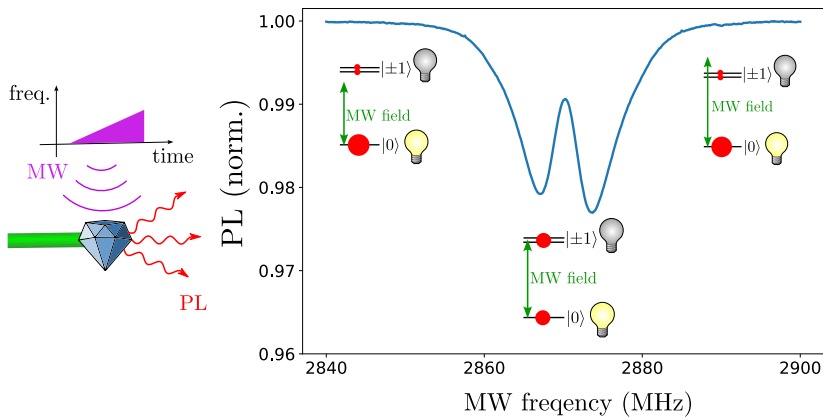
Optically detected magnetic resonance (ODMR)



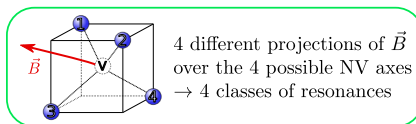
Optically detected magnetic resonance (ODMR)



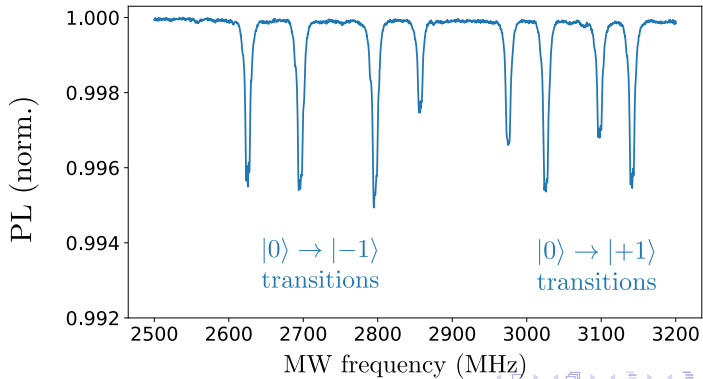
Optically detected magnetic resonance (ODMR)



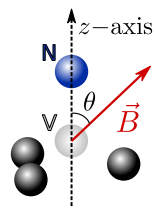
ODMR with NV ensemble: the 4 classes



Position of the 8 lines:
→ 3D reconstruction of \vec{B}



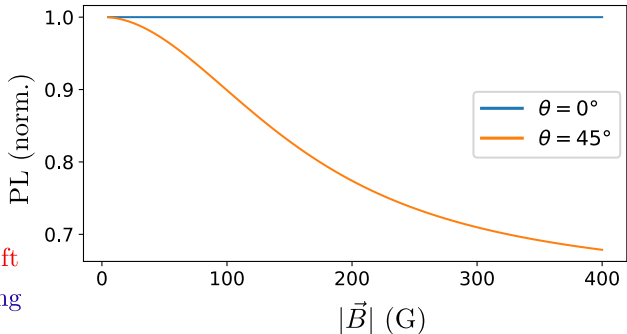
Transverse magnetic field effect



B_{\parallel} = Zeeman shift

B_{\perp} = State mixing

Loss of polarization, PL decrease



Outline

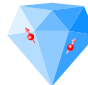
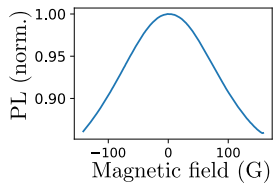
Sensing with quantum mechanics

NV center spin properties

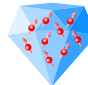
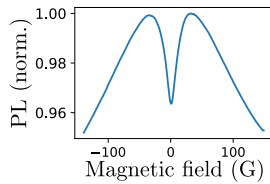
Low field depolarization magnetometry (LFDM)

Depolarization mechanisms in dense NV ensemble

Depolarization of dense NV ensemble at low magnetic field

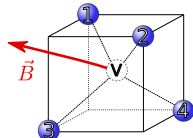


Low NV density
 $[NV] \leq 100$ ppb

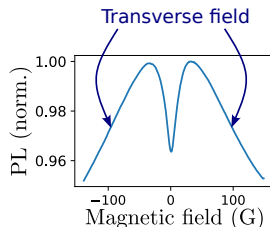
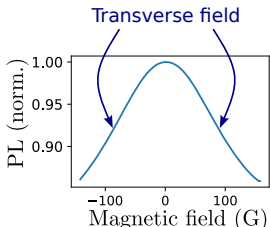


High NV density
 $[NV] \geq 1$ ppm

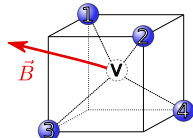
Depolarization of dense NV ensemble at low magnetic field



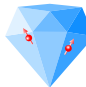
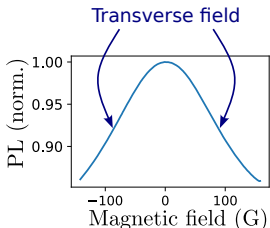
Non-zero transverse
magnetic field
on all 4 classes



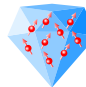
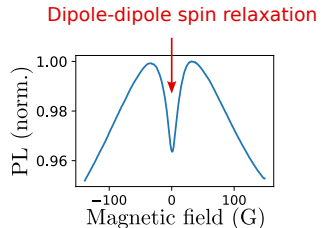
Depolarization of dense NV ensemble at low magnetic field



Non-zero transverse
magnetic field
on all 4 classes

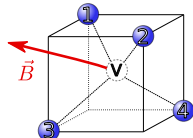


Low NV density
 $[NV] \leq 100$ ppb

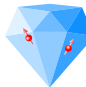
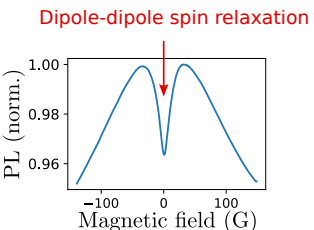
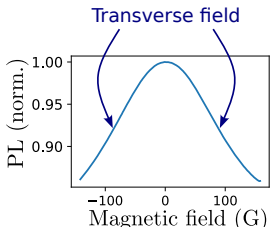


High NV density
 $[NV] \geq 1$ ppm

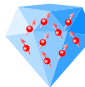
Depolarization of dense NV ensemble at low magnetic field



Non-zero transverse
magnetic field
on all 4 classes



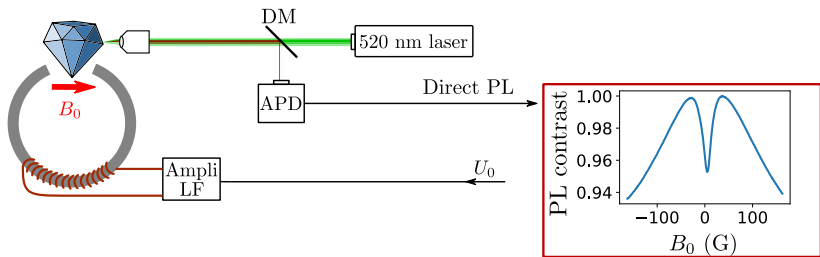
Low NV density
 $[NV] \leq 100$ ppb



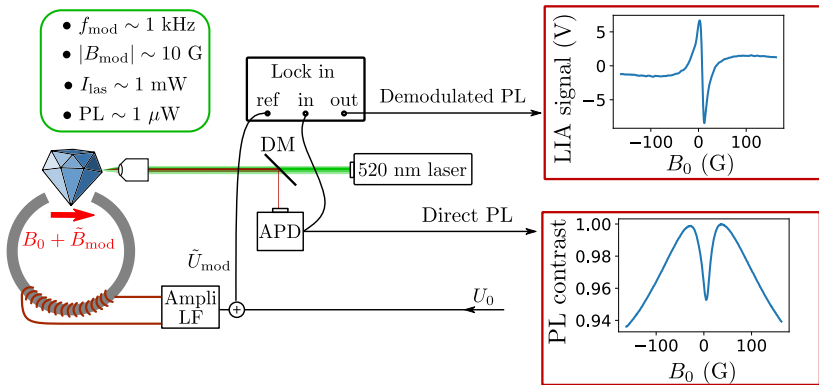
High NV density
 $[NV] \geq 1$ ppm

Sharp PL feature → magnetometry

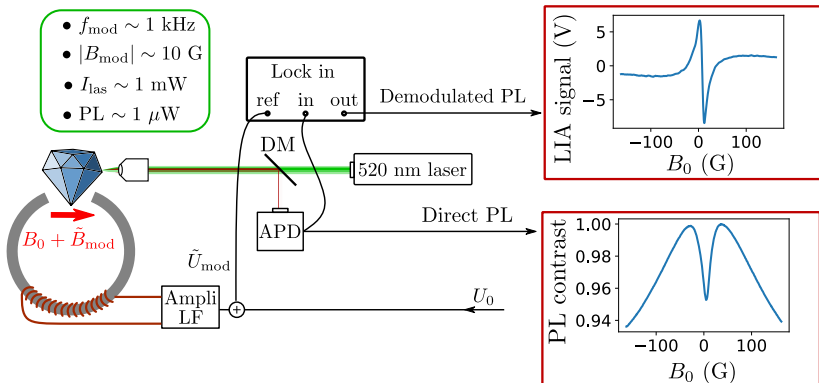
LFDM experimental setup



LFDM experimental setup



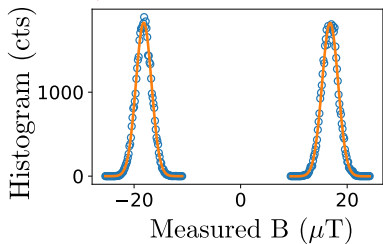
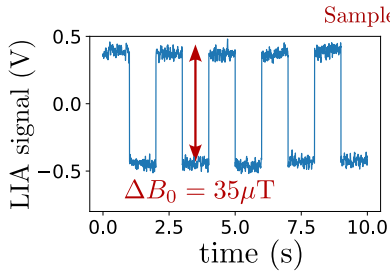
LFDM experimental setup



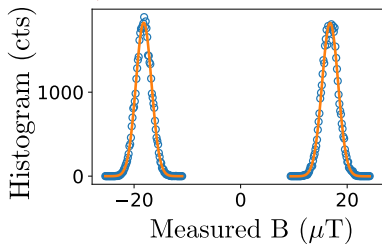
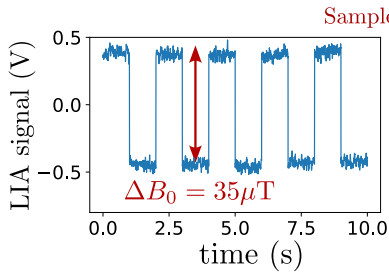
LIA:

- Avoid low frequency noise
- Linear dependance between U_{out} and B_0

Sensitivity of LFDM



Sensitivity of LFDM



Measurement time $\tau = 3 \text{ ms} \quad \sqrt{\langle \delta B^2 \rangle} \approx 1.2 \mu\text{T}$

$$\rightarrow \text{sensitivity } \eta = \sqrt{2\tau \langle \delta B^2 \rangle} \approx 120 \text{ nT}/\sqrt{\text{Hz}}$$

Comparison with the state of the art

Sensitivity comparison

	ODMR [1]	GSLAC [2]	LFDM
η (nT/ $\sqrt{\text{Hz}}$)	0.015	0.3	116

[1] Barry, J. F. [...] Walsworth, R. L (2016). PNAS, 113(49), 14133-14138.

[2] Zheng, H.[...] Budker, D. (2020). Physical Review Applied, 13(4), 044023.

Comparison with the state of the art

Sensitivity comparison

	ODMR [1]	GSLAC [2]	LFDM
η (nT/ $\sqrt{\text{Hz}}$)	0.015	0.3	116
V (μm^3)	$5.2 \cdot 10^6$?	$3.3 \cdot 10^3$
η_v (nT $\mu\text{m}^{3/2}\text{Hz}^{-1/2}$)	34	?	6700

[1] Barry, J. F. [...] Walsworth, R. L (2016). PNAS, 113(49), 14133-14138.

[2] Zheng, H.[...] Budker, D. (2020). Physical Review Applied, 13(4), 044023.

Comparison with the state of the art

Sensitivity comparison

	ODMR [1]	GSLAC [2]	LFDM
η (nT/ $\sqrt{\text{Hz}}$)	0.015	0.3	116
V (μm^3)	$5.2 \cdot 10^6$?	$3.3 \cdot 10^3$
η_v (nT $\mu\text{m}^{3/2}\text{Hz}^{-1/2}$)	34	?	6700

[1] Barry, J. F. [...] Walsworth, R. L (2016). PNAS, 113(49), 14133-14138.

[2] Zheng, H.[...] Budker, D. (2020). Physical Review Applied, 13(4), 044023.

	ODMR	GSLAC	LFDM
Microwave free	✗	✓	✓

Comparison with the state of the art

Sensitivity comparison

	ODMR [1]	GSLAC [2]	LFDM
η (nT/ $\sqrt{\text{Hz}}$)	0.015	0.3	116
V (μm^3)	$5.2 \cdot 10^6$?	$3.3 \cdot 10^3$
η_v (nT $\mu\text{m}^{3/2}\text{Hz}^{-1/2}$)	34	?	6700

[1] Barry, J. F. [...] Walsworth, R. L (2016). PNAS, 113(49), 14133-14138.

[2] Zheng, H.[...] Budker, D. (2020). Physical Review Applied, 13(4), 044023.

	ODMR	GSLAC	LFDM
Microwave free	✗	✓	✓
Low magnetic field (<10 G)	✓	✗	✓

Comparison with the state of the art

Sensitivity comparison

	ODMR [1]	GSLAC [2]	LFDM
η (nT/ $\sqrt{\text{Hz}}$)	0.015	0.3	116
V (μm^3)	$5.2 \cdot 10^6$?	$3.3 \cdot 10^3$
η_v (nT $\mu\text{m}^{3/2}\text{Hz}^{-1/2}$)	34	?	6700

[1] Barry, J. F. [...] Walsworth, R. L (2016). PNAS, 113(49), 14133-14138.

[2] Zheng, H.[...] Budker, D. (2020). Physical Review Applied, 13(4), 044023.

	ODMR	GSLAC	LFDM
Microwave free	✗	✓	✓
Low magnetic field (<10 G)	✓	✗	✓
Robust to T° and B-field inhomogeneities	✗	✗	✓

Comparison with the state of the art

Sensitivity comparison

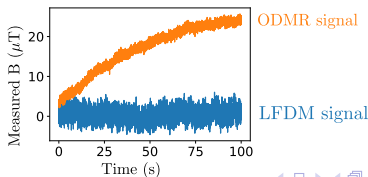
	ODMR [1]	GSLAC [2]	LFDM
η (nT/ $\sqrt{\text{Hz}}$)	0.015	0.3	116
V (μm^3)	$5.2 \cdot 10^6$?	$3.3 \cdot 10^3$
η_v (nT $\mu\text{m}^{3/2}\text{Hz}^{-1/2}$)	34	?	6700

[1] Barry, J. F. [...] Walsworth, R. L (2016). PNAS, 113(49), 14133-14138.

[2] Zheng, H.[...] Budker, D. (2020). Physical Review Applied, 13(4), 044023.

	ODMR	GSLAC	LFDM
Microwave free	✗	✓	✓
Low magnetic field (<10 G)	✓	✗	✓
Robust to T° and B-field inhomogeneities	✗	✗	✓

Temporal trace
for fixed B_0



Comparison with the state of the art

Sensitivity comparison

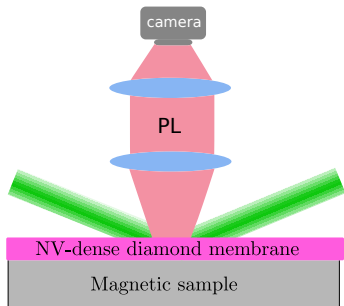
	ODMR [1]	GSLAC [2]	LFDM
η (nT/ $\sqrt{\text{Hz}}$)	0.015	0.3	116
V (μm^3)	$5.2 \cdot 10^6$?	$3.3 \cdot 10^3$
η_v (nT $\mu\text{m}^{3/2}\text{Hz}^{-1/2}$)	34	?	6700

[1] Barry, J. F. [...] Walsworth, R. L (2016). PNAS, 113(49), 14133-14138.

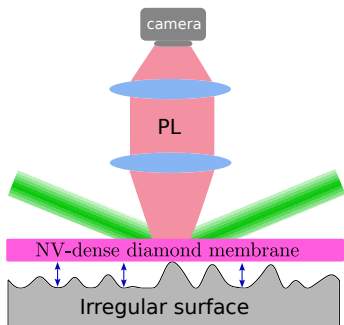
[2] Zheng, H.[...] Budker, D. (2020). Physical Review Applied, 13(4), 044023.

	ODMR	GSLAC	LFDM
Microwave free	✗	✓	✓
Low magnetic field (<10 G)	✓	✗	✓
Robust to T° and B-field inhomogeneities	✗	✗	✓
Orientation free (polycrystalline, powder)	✗	✗	✓

Application: wide-field magnetometry

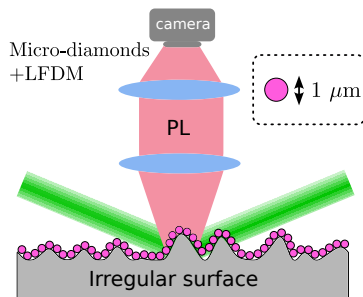
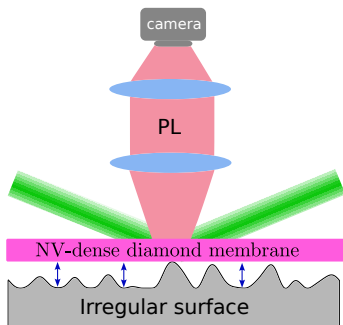


Application: wide-field magnetometry

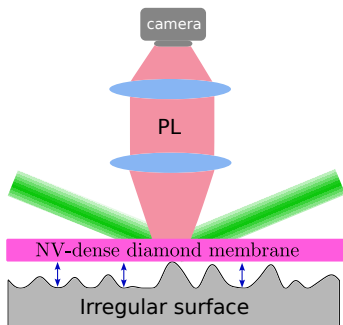


Gaps: loss of spatial resolution

Application: wide-field magnetometry



Application: wide-field magnetometry

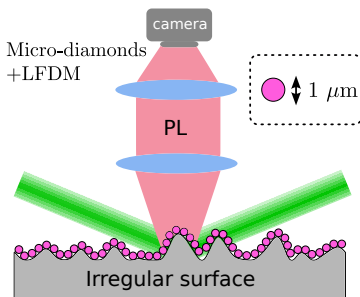


Gaps: loss of spatial resolution

State of the art [1]:

Area normalized sensitivity:
 $\eta_S \approx 20 \mu\text{T} \cdot \mu\text{m}/\sqrt{\text{Hz}}$

[1] Glenn, D. R. [...] Walsworth, R. L. (2017) *Geochemistry, Geophysics, Geosystems*, 18(8), 3254–3267.



LFDM :

Area normalized sensitivity:
 $\eta_S \approx 6 \mu\text{T} \cdot \mu\text{m}/\sqrt{\text{Hz}}$

Outline

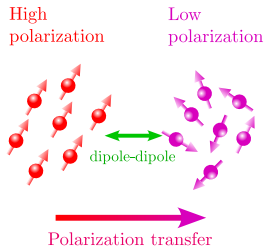
Sensing with quantum mechanics

NV center spin properties

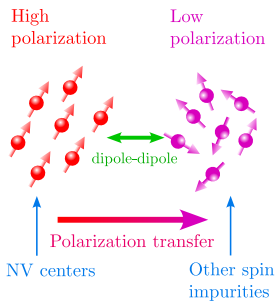
Low field depolarization magnetometry (LFDM)

Depolarization mechanisms in dense NV ensemble

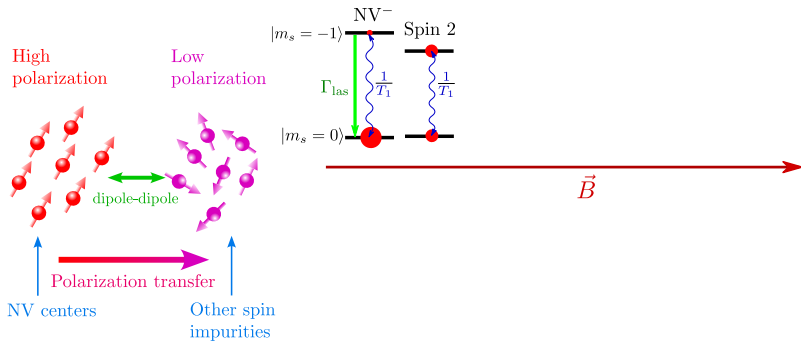
Principle of cross-relaxation with NV centers



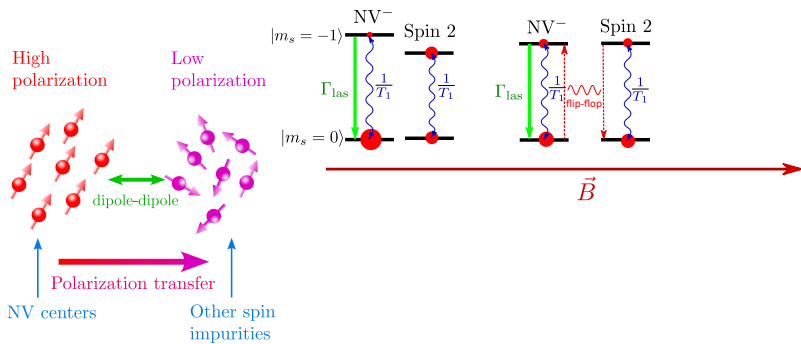
Principle of cross-relaxation with NV centers



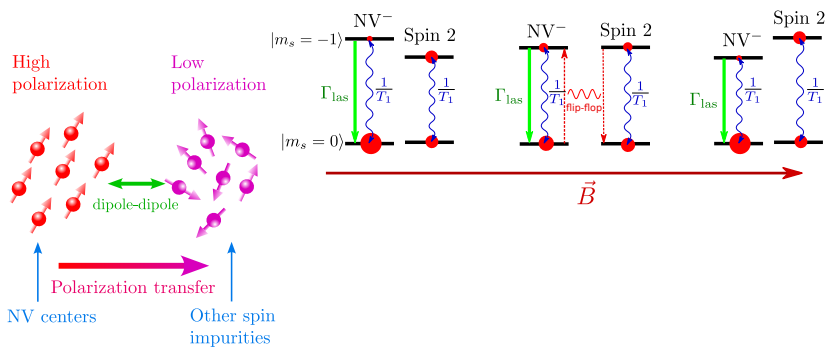
Principle of cross-relaxation with NV centers



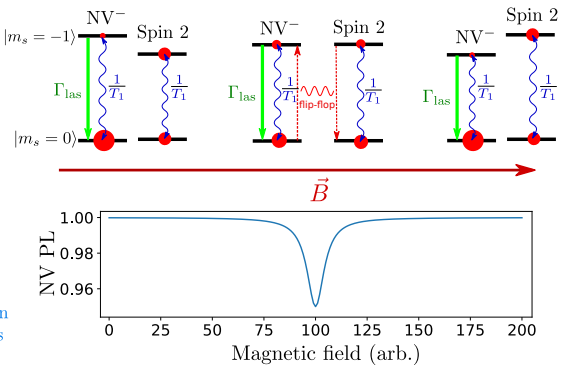
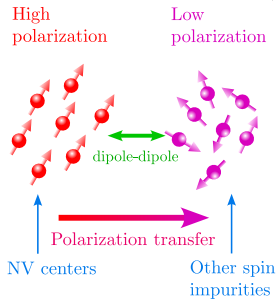
Principle of cross-relaxation with NV centers



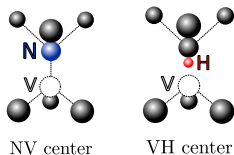
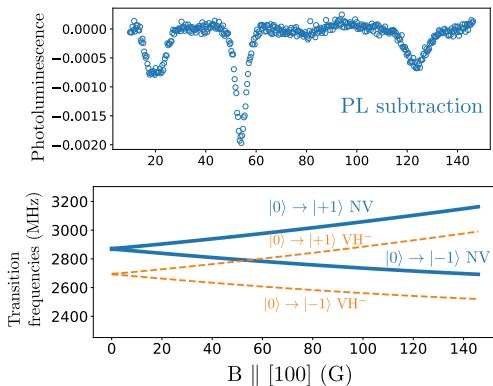
Principle of cross-relaxation with NV centers



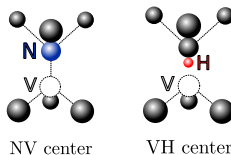
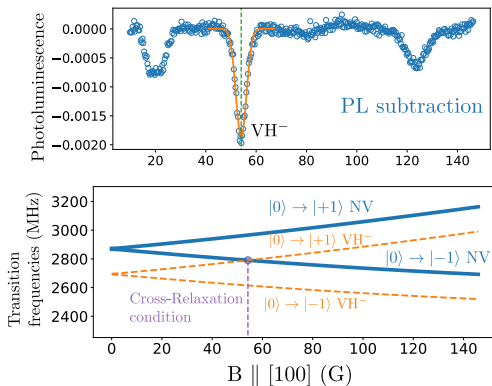
Principle of cross-relaxation with NV centers



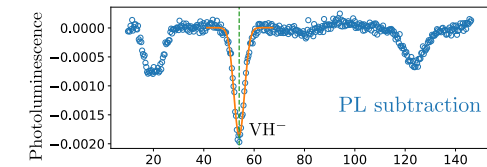
Example: Cross-relaxation between NV centers and VH⁻



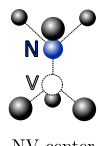
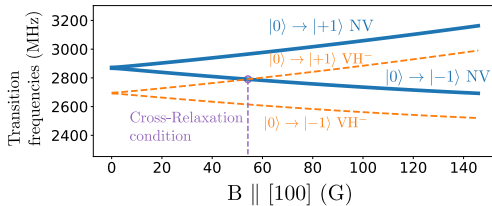
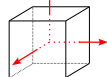
Example: Cross-relaxation between NV centers and VH⁻



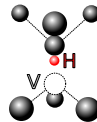
Example: Cross-relaxation between NV centers and VH⁻



$$\vec{B} \parallel \langle 100 \rangle$$

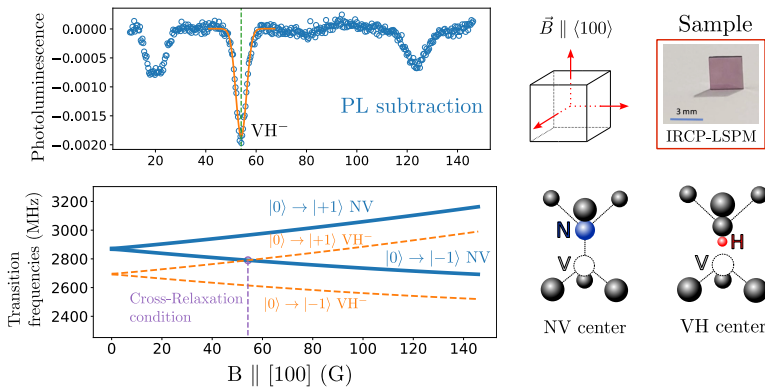


NV center

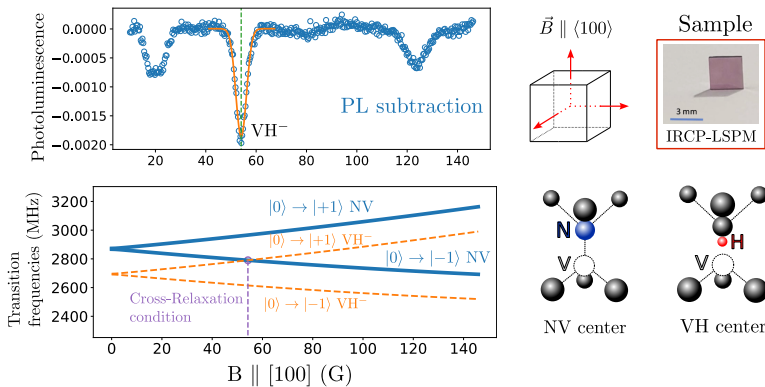


VH center

Example: Cross-relaxation between NV centers and VH⁻



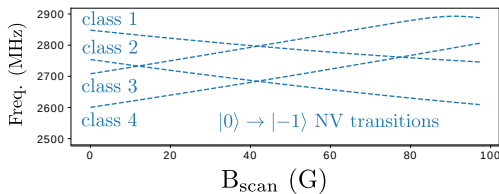
Example: Cross-relaxation between NV centers and VH⁻



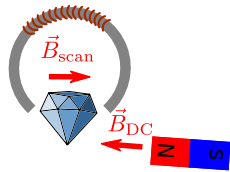
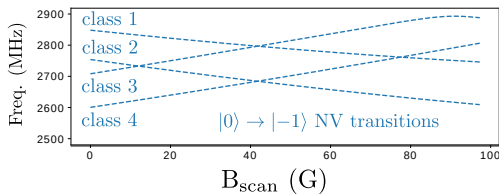
Optical detection of paramagnetic defects in diamond grown by chemical vapor deposition

C. Pellet-Mary, P. Huillery, M. Perdriat, A. Tallaire, and G. Hétet
Phys. Rev. B **103**, L100411 – Published 24 March 2021

Cross-relaxation between NV centers and NV centers

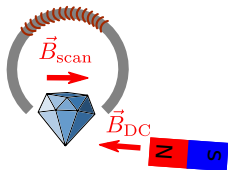
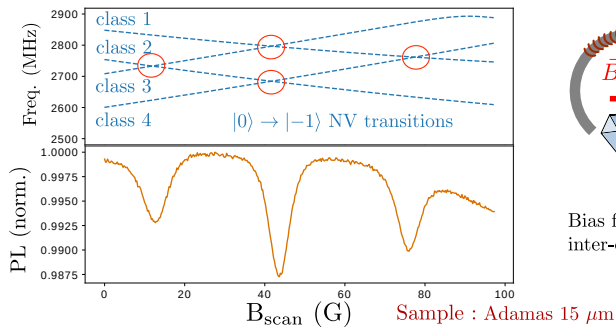


Cross-relaxation between NV centers and NV centers



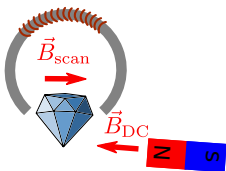
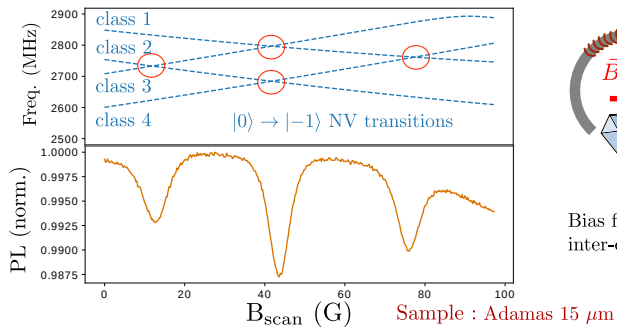
Bias field required to create inter-class resonances

Cross-relaxation between NV centers and NV centers

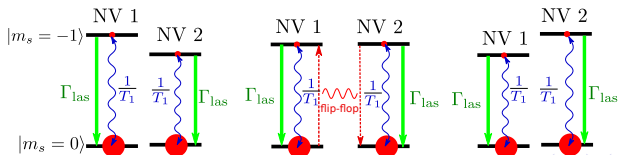


Bias field required to create inter-class resonances

Cross-relaxation between NV centers and NV centers



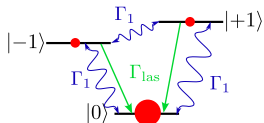
Bias field required to create inter-class resonances



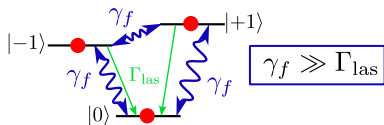
Problem:
no CR for equally
polarized spins

Presentation of the fluctuator model

Normal NV



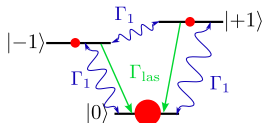
Fluctuator NV



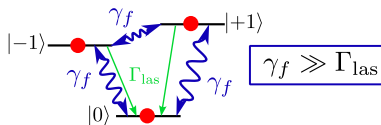
Choi, J. [...] Lukin, M. D. (2017). PRL, 118(9), 093601.

Presentation of the fluctuator model

Normal NV



Fluctuator NV



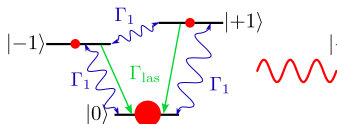
Fluctuators:

- Same spin levels as NV centers
- Unpolarized

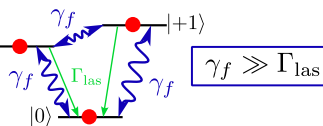
Choi, J. [...] Lukin, M. D. (2017). PRL, 118(9), 093601.

Presentation of the fluctuator model

Normal NV



Fluctuator NV



~~NV-NV Cross-relaxation~~
 \rightarrow NV-fluct Cross-relaxation

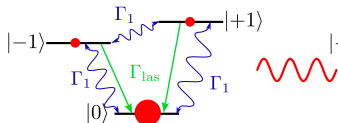
Fluctuators:

- Same spin levels as NV centers
- Unpolarized

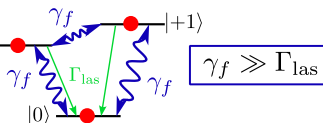
Choi, J. [...] Lukin, M. D. (2017). PRL, 118(9), 093601.

Presentation of the fluctuator model

Normal NV



Fluctuator NV



~~NV-NV Cross-relaxation~~
→ NV-fluct Cross-relaxation

Fluctuators:

- Same spin levels as NV centers
- Unpolarized

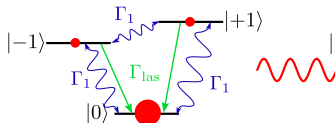
Precedents in:

- P-doped Si
- Solid-state NMR
- FRET

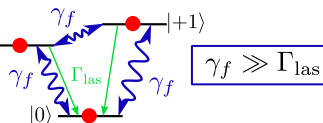
Choi, J. [...] Lukin, M. D. (2017). PRL, 118(9), 093601.

Presentation of the fluctuator model

Normal NV



Fluctuator NV



~~NV-NV Cross-relaxation~~
→ NV-fluct Cross-relaxation

Precedents in:

- P-doped Si
- Solid-state NMR
- FRET

Fluctuators:

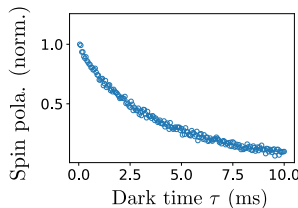
- Same spin levels as NV centers
- Unpolarized

Potential microscopic origin:

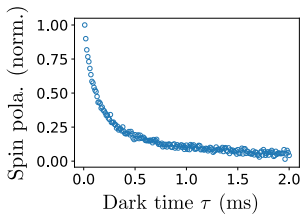
- Charge tunneling
 - Modulation of contact interaction
- Fluctuator = impurity cluster

Choi, J. [...] Lukin, M. D. (2017). PRL, 118(9), 093601.

Stretched exponential decay profile

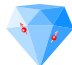
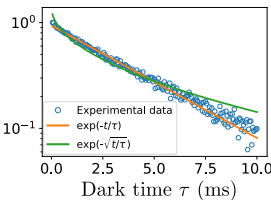
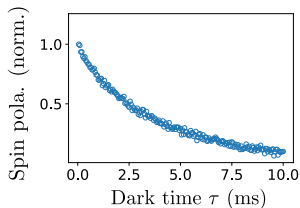


Low NV density
• $T_1 \sim 5$ ms



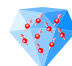
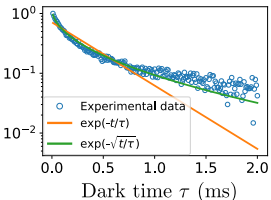
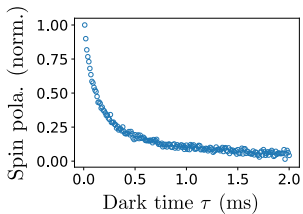
High NV density
• $T_1 \sim 0.5$ ms

Stretched exponential decay profile



Low NV density

- $T_1 \sim 5$ ms
- Exponential profile

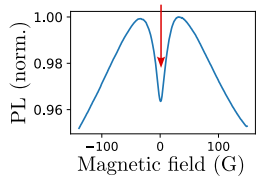


High NV density

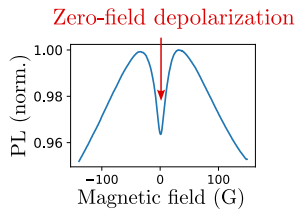
- $T_1 \sim 0.5$ ms
- Stretched exp. profile

Zero field depolarization mechanisms (theory)

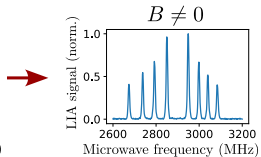
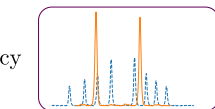
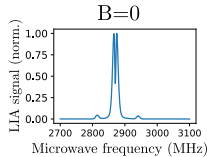
Zero-field depolarization



Zero field depolarization mechanisms (theory)



- 4-classes degeneracy

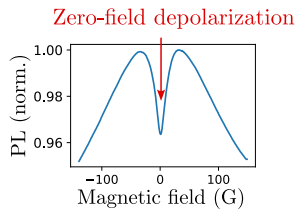


Increased magnetic field

→ lift of the 4 classes degeneracy

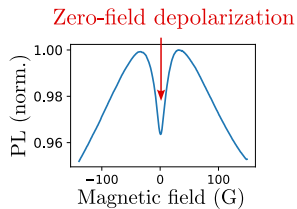
→ reduction of spin exchange

Zero field depolarization mechanisms (theory)



- 4-classes degeneracy
 - Eigenbasis change
- $$|\pm\rangle = \frac{|+1\rangle \pm |-1\rangle}{\sqrt{2}}$$
- New eigenstates in zero-field
 → new dipole-dipole coupling rates
 → increased depolarization in zero-field

Zero field depolarization mechanisms (theory)



- 4-classes degeneracy
 - Eigenbasis change
 - Double flips
- Flip-flops**

$$|{-1}, 0\rangle \rightarrow |0, {-1}\rangle$$

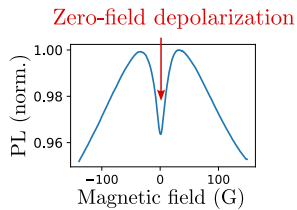
Always resonant

Double flips

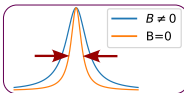
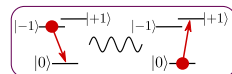
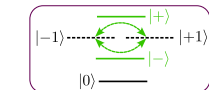
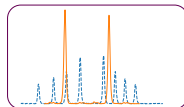
$$|{-1}, 0\rangle \rightarrow |0, +1\rangle$$

Only resonant in 0B

Zero field depolarization mechanisms (theory)

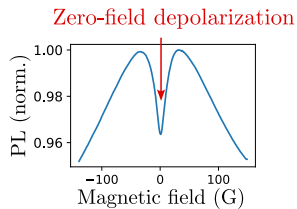


- 4-classes degeneracy
- Eigenbasis change
- Double flips
- T_2^* increase

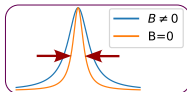
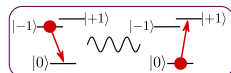
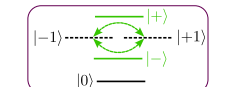
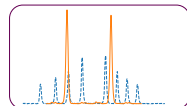


Lower spectral linewidth → Higher coupling rate

Zero field depolarization mechanisms (theory)



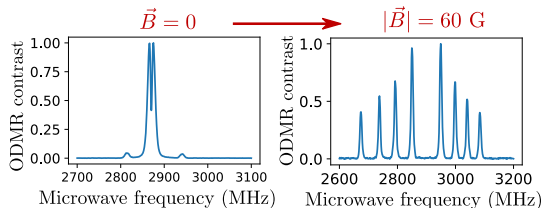
- 4-classes degeneracy
- Eigenbasis change
- Double flips
- T_2^* increase



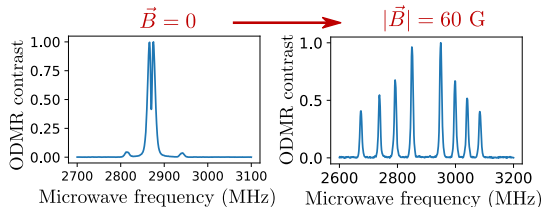
Relative contribution (numerical):

4 classes-degeneracy \gg Double-flips $>$ Eigenbasis change $\approx T_2^*$ increase

Experiment: \vec{B} in arbitrary direction

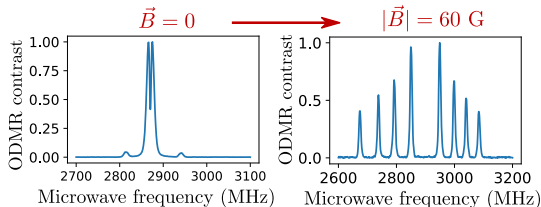


Experiment: \vec{B} in arbitrary direction

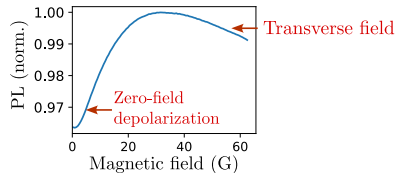


- 4-classes degeneracy
- Eigenbasis change
- Double-flips
- T_2^* change

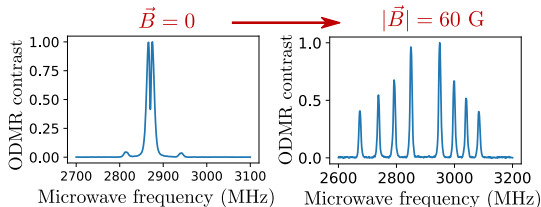
Experiment: \vec{B} in arbitrary direction



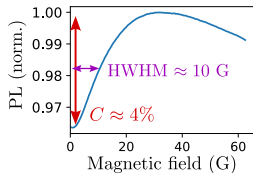
- 4-classes degeneracy
- Eigenbasis change
- Double-flips
- T_2^* change



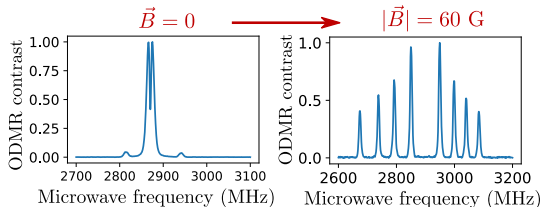
Experiment: \vec{B} in arbitrary direction



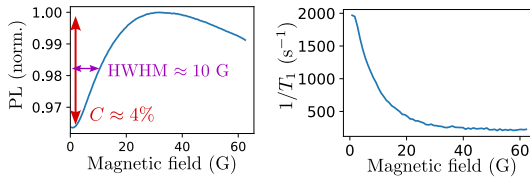
- 4-classes degeneracy
- Eigenbasis change
- Double-flips
- T_2^* change



Experiment: \vec{B} in arbitrary direction

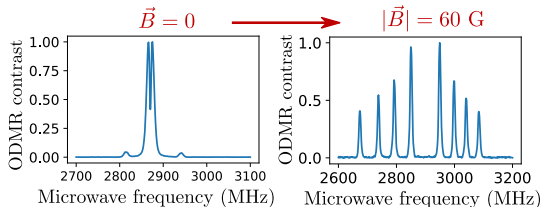


- 4-classes degeneracy
- Eigenbasis change
- Double-flips
- T_2^* change

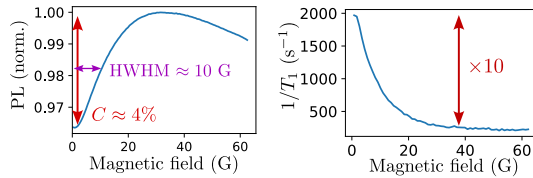


T_1 measured for each magnetic field values

Experiment: \vec{B} in arbitrary direction

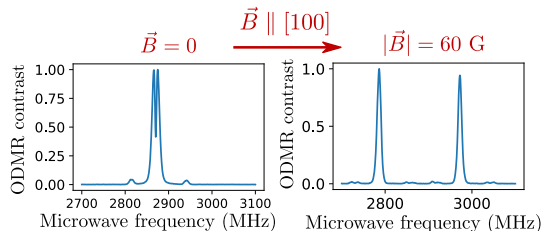


- 4-classes degeneracy
- Eigenbasis change
- Double-flips
- T_2^* change

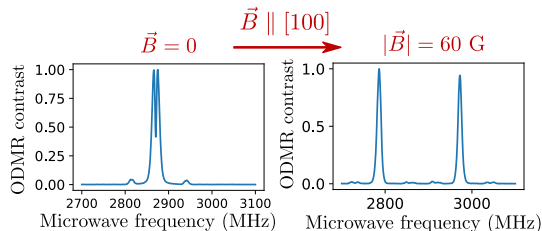


Depolarization increased by $\sim \times 10$ in zero magnetic field

Experiment: $\vec{B} \parallel [100]$

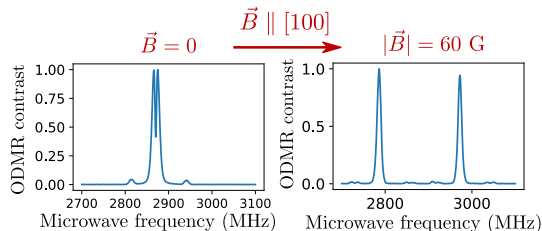


Experiment: $\vec{B} \parallel [100]$

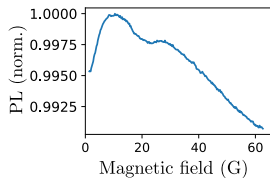


- 4 classes degeneracy
- Eigenbasis change
- Double-flips
- T_2^* change

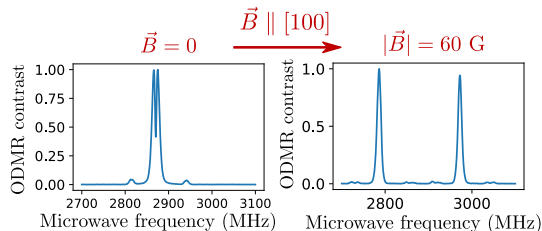
Experiment: $\vec{B} \parallel [100]$



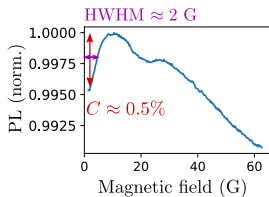
- 4 classes degeneracy
- Eigenbasis change
- Double-flips
- T_2^* change



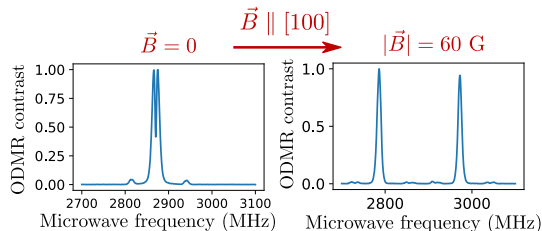
Experiment: $\vec{B} \parallel [100]$



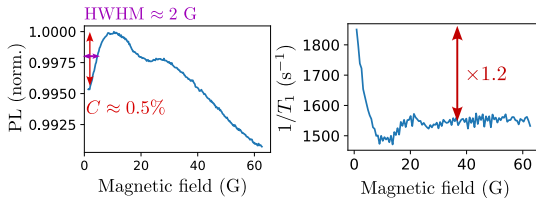
- 4 classes degeneracy
- Eigenbasis change
- Double-flips
- T_2^* change



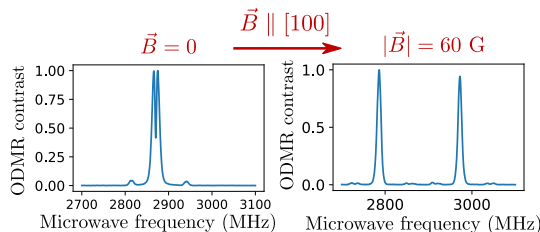
Experiment: $\vec{B} \parallel [100]$



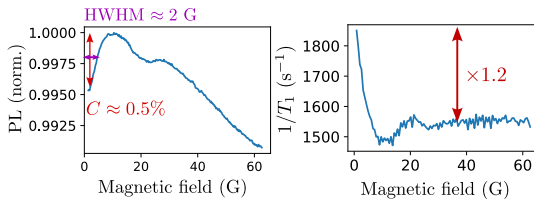
- 4 classes degeneracy
- Eigenbasis change
- Double-flips
- T_2^* change



Experiment: $\vec{B} \parallel [100]$

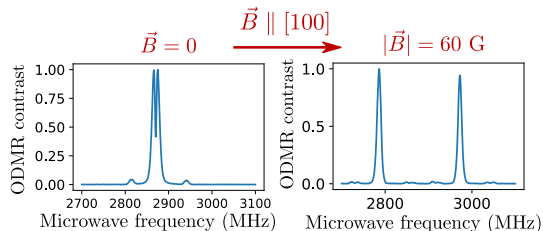


- 4 classes degeneracy
- Eigenbasis change
- Double-flips
- T_2^* change

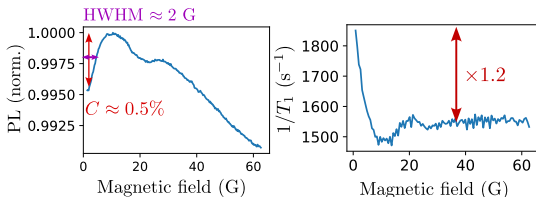


Depolarization
increased by $\sim \times 1.2$
in zero magnetic field

Experiment: $\vec{B} \parallel [100]$



- 4-classes degeneracy
- Eigenbasis change
- Double-flips
- T_2^* change



Depolarization increased by $\sim \times 1.2$ in zero magnetic field

4-classes degeneracy dominates low-field depolarization

Conclusion

- ▶ The use of NV center ensemble for magnetometry is currently limited by the interactions between the spin defects.

Conclusion

- ▶ The use of NV center ensemble for magnetometry is currently limited by the interactions between the spin defects.
- ▶ Dipole-dipole interaction within dense ensemble of NV centers result in spin depolarization. This effect is stronger in zero-field.

Conclusion

- ▶ The use of NV center ensemble for magnetometry is currently limited by the interactions between the spin defects.
- ▶ Dipole-dipole interaction within dense ensemble of NV centers result in spin depolarization. This effect is stronger in zero-field.
- ▶ This depolarization can be used to perform microwave-free and orientation-free magnetometry at low magnetic field.

Conclusion

- ▶ The use of NV center ensemble for magnetometry is currently limited by the interactions between the spin defects.
- ▶ Dipole-dipole interaction within dense ensemble of NV centers result in spin depolarization. This effect is stronger in zero-field.
- ▶ This depolarization can be used to perform microwave-free and orientation-free magnetometry at low magnetic field.
- ▶ The physics of low-field depolarization is complex and need to be further studied to improve the performances of LFDM.

Acknowledgments

Diamond team

Gabriel Hétet

Maxime Perdriat

Paul Huillery

Tom Delord

Louis Nicolas

Nano-optics

Christophe Voisin

Carole Diederichs

Yannick Chassagneux

Emmanuel Baudin

Christos Flytzanis

Technical Staff

Pascal Morfin

Arnaud Leclerq

Nabil Garroum

Didier Courtiade

IRCP/LSPM

Alexandre Tallaire

Philippe Goldner

Jocelyn Achard

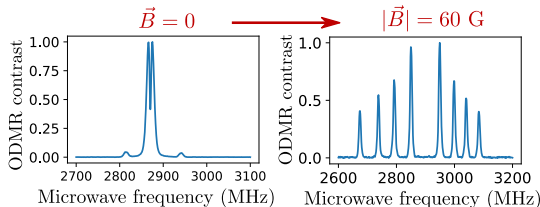
Midrel Ngandeu Ngambo

Administrative staff

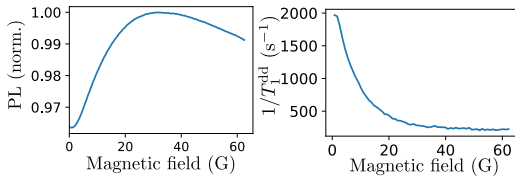
Olga Hodges

Christine Chambon

Experiment: \vec{B} in arbitrary direction

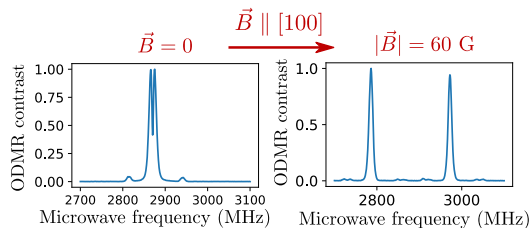


- 4-classes degeneracy
- Eigenbasis change
- Double-flips
- T_2^* change

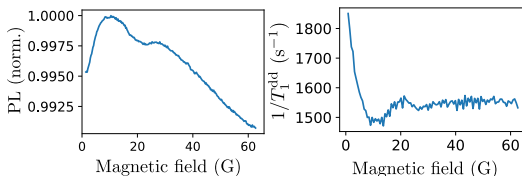


$\Gamma_1(B = 0) \approx 10 \Gamma_1(B \neq 0)$
 $\sim 4\%$ PL contrast
HWHM ~ 9 G

Experiment: $\vec{B} \parallel [100]$



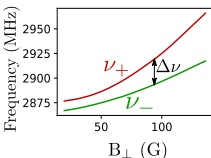
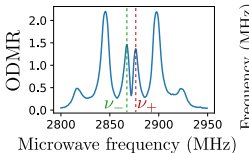
- 4-classes degeneracy
- Eigenbasis change
- Double-flips
- T_2^* change



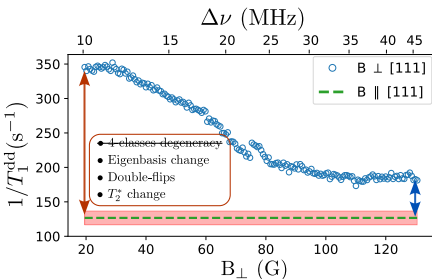
$\Gamma_1(B = 0) \approx 1.2 \Gamma_1(B \neq 0)$
 $\sim 0.5\%$ PL contrast
 HWHM ~ 2 G

Classes degeneracy is the dominant cause of depolarization at low magnetic field

Experiment: $\vec{B} \perp [111]$



Same eigenbasis :
 $|\pm\rangle = \frac{|+1\rangle \pm |-1\rangle}{\sqrt{2}}$
 for $\vec{B} \perp [111]$ than for $\vec{B} = 0$



cancelling out double flips
with transverse field

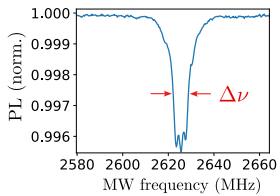
- 4 classes degeneracy
- Eigenbasis change
- Double-flips
- T_2^* change

Double flips are the second dominant cause
of depolarization at low magnetic field

NV center magnetometry sensitivity

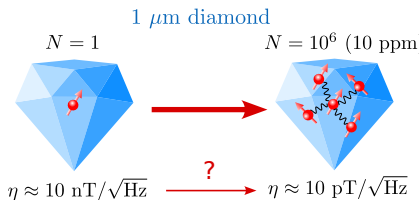
Ideal (DC) sensitivity for
 N independent NV centers:

$$\eta[T/\sqrt{\text{Hz}}] \approx \frac{\hbar\sqrt{\Delta\nu}}{g\mu_B C\sqrt{N}}$$

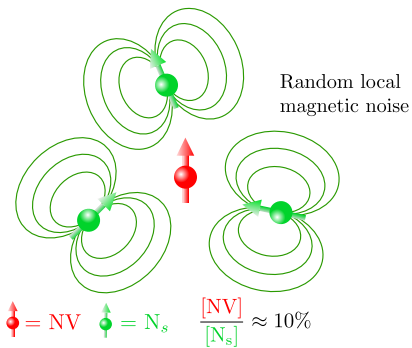


- \hbar : Planck constant
 - μ_B : Bohr magneton
 - g : NV electron Landé factor
 - C : Spin readout contrast
 - N : Number of NV centers
 - $\Delta\nu = \frac{1}{T_2^*}$: Spectral linewidth
- Constants

Experimental parameters
- Sample parameters

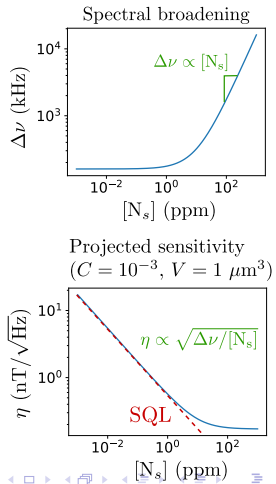


NV center magnetometry: the interaction limit



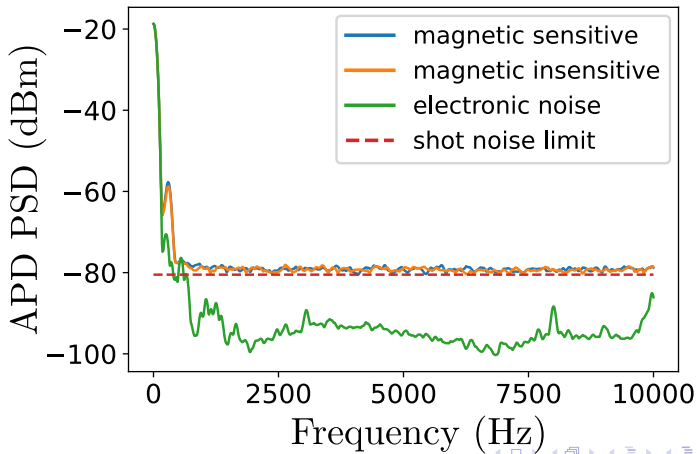
Going beyond the “Interaction limit” ($[N_s] > 10$ ppm):

- Decoupling interaction (Hamiltonian engineering)
 - Exploiting interactions

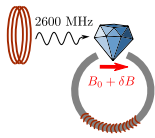


LFDM: shot-noise limit

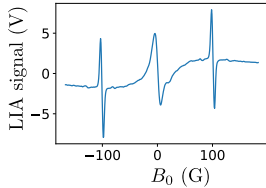
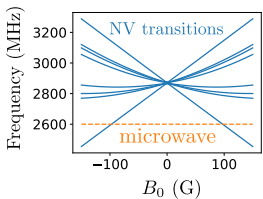
$$PL \sim 1 \mu\text{W} \sim 10^{12} \text{ photons/s}$$



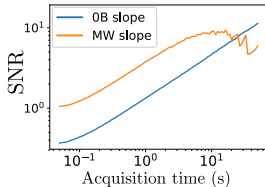
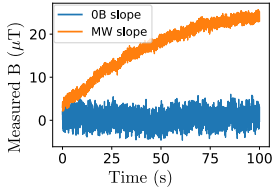
Comparison with CW ODMR



Adding a fixed microwave tone



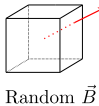
Temporal stability



$$\text{MW slope sensitivity: } \eta \approx 40 \text{ nT}/\sqrt{\text{Hz}}$$

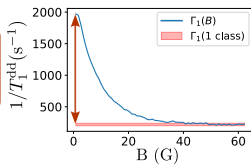
$$B=0 \text{ sensitivity: } \eta \approx 120 \text{ nT}/\sqrt{\text{Hz}}$$

Summary of the experimental observations

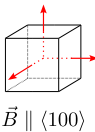


Random \vec{B}

- 4-classes degeneracy
- Eigenbasis change
- Double-flips
- T_2^* change

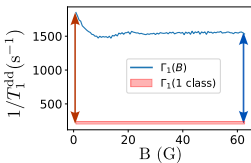


- 4-classes degeneracy
- Eigenbasis change
- Double-flips
- T_2^* change

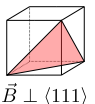


$\vec{B} \parallel \langle 100 \rangle$

- 4-classes degeneracy
- Eigenbasis change
- Double-flips
- T_2^* change

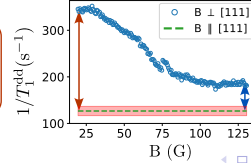


- 4-classes degeneracy
- Eigenbasis change
- Double-flips
- T_2^* change



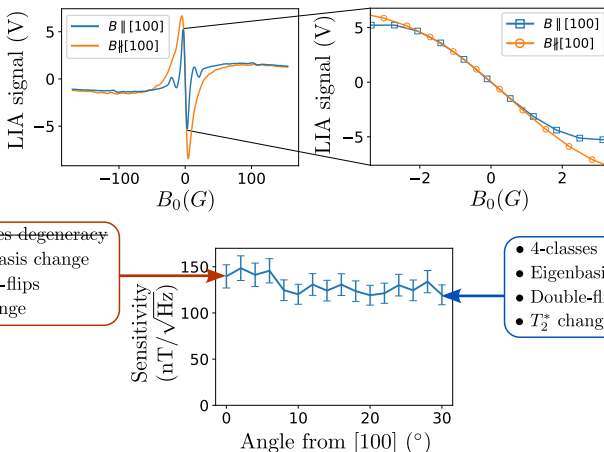
$\vec{B} \perp \langle 111 \rangle$

- 4-classes degeneracy
- Eigenbasis change
- Double-flips
- T_2^* change



- 4-classes degeneracy
- Eigenbasis change
- Double-flips
- T_2^* change

Angular sensitivity of LFDM



The 4-classes degeneracy is not the limiting factor of the sensitivity